



# Erosion and deposition at the ALT-II limiter of TEXTOR

M. Mayer <sup>a,\*</sup>, P. Wienhold <sup>b</sup>, D. Hildebrandt <sup>c</sup>, W. Schneider <sup>c</sup>

<sup>a</sup> *Max-Planck-Institut für Plasmaphysik, EURATOM Association, Boltzmannstr. 2, D-85748 Garching, Germany*

<sup>b</sup> *Institut für Plasmaphysik, FZ Jülich GmbH, Trilateral Euregio Cluster, EURATOM Association, D-52425 Jülich, Germany*

<sup>c</sup> *Max-Planck-Institut für Plasmaphysik, EURATOM Association, Mohrenstr. 41, D-10117 Berlin, Germany*

## Abstract

A new method for the determination of massive erosion and deposition on plasma facing components has been developed and was tested successfully on a graphite tile of the ALT-II limiter of TEXTOR. The surface profile of the tile was measured before and after exposure to plasma discharges with an optical profiler, erosion or deposition is determined from the difference of the two profiles. The profiles were determined relative to specially machined holes, which provide stable reference points. An accuracy of about 1  $\mu\text{m}$  can be achieved. After exposure for 7625 plasma seconds a maximum erosion of 28  $\mu\text{m}$  carbon is observed in erosion dominated areas, while a maximum deposition of about 40  $\mu\text{m}$  is observed in net redeposition areas. The composition and structure of the redeposited layers were investigated with secondary ion mass spectroscopy and scanning electron microscopy.

© 2003 Elsevier Science B.V. All rights reserved.

PACS: 52.40.Hf

Keywords: Erosion measurement; Redeposition; TEXTOR; Limiter; Profilometry; Deuterium inventory

## 1. Introduction

In nuclear fusion devices hydrogen isotopes are mainly accumulated in codeposited layers together with eroded and redeposited carbon atoms [1]. The accumulation of tritium in these layers is a major safety problem for ITER [2]. For a quantitative understanding of erosion and redeposition phenomena measurements in today's experiments are necessary. In areas with major plasma contact, such as divertor or limiter tiles, the thickness of redeposited layers may reach tens or even hundreds of microns during one year of operation [1,3,4]. The quantitative analysis of such massive deposits is an analytical challenge: Layer thicknesses up to about 15  $\mu\text{m}$  can be analyzed with ion beam analysis techniques using high energetic incident protons [5], even thicker layers can be analyzed with secondary ion mass spectroscopy (SIMS). If the deposited layer is

flaking off the substrate, flake thicknesses can be determined with scanning electron microscopy (SEM) [6].

But none of these techniques is able to determine erosion. Small erosion of the order of several 100 nm has been determined by colorimetry [7], or by using thin layers of different materials, which thicknesses were analyzed before and after plasma exposure [8]. These methods run into severe difficulties, however, if layer thicknesses exceed several  $\mu\text{m}$  due to adhesion and technological problems. Very massive erosion ( $>100 \mu\text{m}$ ) has been measured using a three-dimensional coordinate measuring machine [9], but this method is not sufficiently accurate to determine erosion of the order of several 10  $\mu\text{m}$ . The most promising technique for the determination of erosion in this range is speckle interferometry [10], but this technique has failed to prove its utilisability in the harsh environment of a nuclear fusion experiment.

The lack of applicable methods for the determination of erosion at the areas with major plasma contact, such as limiters or divertor strike points, is a major drawback and results in severe uncertainties about the source of

\* Corresponding author. Tel.: +49-89 3299 1637; fax: +49-89 3299 2279.

E-mail address: [matej.mayer@ipp.mpg.de](mailto:matej.mayer@ipp.mpg.de) (M. Mayer).

eroded material. In this paper we report about a new method which allows to measure massive erosion. The method was successfully applied to determine erosion at the ALT-II limiter of TEXTOR.

## 2. Experimental

TEXTOR is a medium sized tokamak (minor radius 0.46 m, major radius 1.75 m) with a typical pulse length of about 6 s. The toroidal pumped ALT-II belt limiter (advanced limiter test) consists of 224 graphite tiles mounted on 8 blades, carrying  $2 \times 14$  tiles each. An instrumented tile (tile 20, blade 5) was exposed from February 25 until August 28, 2000 for 7625 plasma seconds, of which 2589 s were ohmic discharges and 5036 s were additionally heated with NI or/and ICRH. Three boronizations were performed during this exposure on March 10, April 28 and June 30. During each boronization about 100 nm a-B:D layer are deposited on the whole inner wall. The wall and limiter temperatures were 200–300 °C.

The instrumented tile 20 is shown in Fig. 1 in its mounting position inside TEXTOR. The tile surface was polished to a mean roughness of about 1  $\mu\text{m}$  and  $3 \times 9$  holes with a diameter of 5 mm, a depth of 0.15–0.45 mm and a poloidal distance of 15 mm were machined into the surface. In order to minimize erosion in the holes the ratio depth/width of the holes was selected in such a

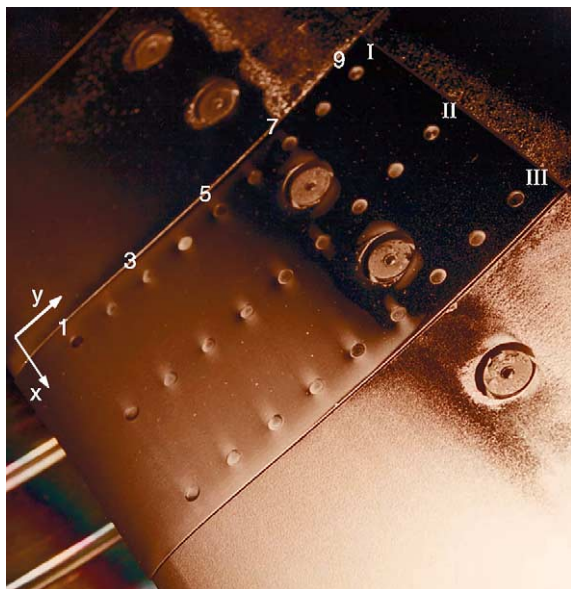


Fig. 1. View of tile 20 after 15 weeks of operation on 13.6.2000. The tile size is  $96 \times 154 \text{ mm}^2$ . The 27 holes are arranged in 9 rows (numbered 1–9) and 3 columns (numbered I–III).  $x$  is in toroidal,  $y$  in poloidal direction.

way, that the hole bottoms are not hit directly by ions which follow the magnetic field lines having an inclination angle of  $1\text{--}2^\circ$  towards the surface. The hole bottoms can be reached only by neutral particles. As a marker of the original surface the hole bottoms were covered with a thin layer of about 200 nm tungsten by magnetron sputter deposition before the plasma exposure. In that way, both, the surface erosion and the material deposition in the holes can be identified by surface layer analysis after the plasma exposure.

The shape of the tile surface was determined with an optical profiler (UBM Microfocus) with a lateral resolution of 100 points/mm for each row in toroidal direction (direction  $x$  in Fig. 1). The vertical resolution of the profiler is about 50 nm with a beam spot diameter of about 1  $\mu\text{m}$ . The profile was determined through the hole centers with an accuracy in poloidal direction (direction  $y$  in Fig. 1) of about 0.025 mm. This accuracy was obtained due to a conical shape of the hole bottoms, the tip of the cone was clearly visible in an optical microscope attached to the profiler.

Surface analysis has been done with SIMS combined with sputter depth profiling. As primary ions 10 keV  $\text{O}_2^+$  ions were used. The depth scale in these measurements was calibrated by profiling the sputter crater. The accuracy of this scale is estimated to be about 15%.

## 3. Results and discussion

### 3.1. Erosion and deposition on tile 20

The SIMS-measurements performed in the holes have shown that the tungsten layer in all holes is completely maintained indicating negligible erosion. On this tungsten layer different amounts of deposited material consisting mainly of carbon and deuterium were found. The thin transition layer is characterized by a strong decrease of the deuterium signal and increase of the tungsten signal. The high deuterium content in the deposited material also allowed to determine the thickness of the deposited layer outside of the holes. The thickness of the deposited layer inside and outside the holes of column II, as derived from the SIMS measurements, is shown in Fig. 2. The measurements were performed in the centers of the holes (inside) or 1 mm above the holes (outside). No deposition is observed outside of rows 1–5, i.e. this region is erosion dominated. At row 6 the transition to a deposition dominated region occurs, and deposition up to 11  $\mu\text{m}$  is observed outside of rows 7–9. In contrast to the observed erosion outside of the holes there is always deposition in the holes, which ranges from 0.7  $\mu\text{m}$  in row 1 to 32  $\mu\text{m}$  in row 9. Note that already the smallest hole recess of 0.15 mm is sufficient to transform an erosion dominated area to a deposition

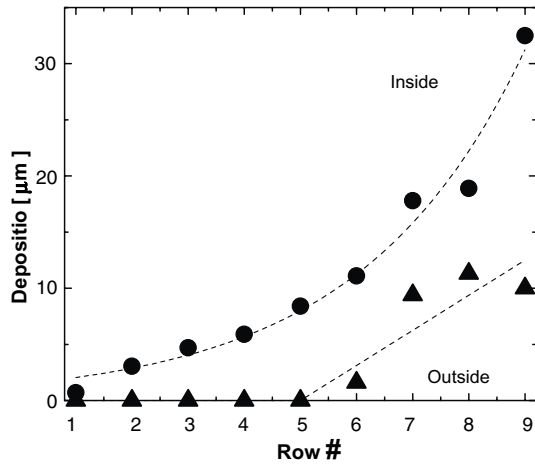


Fig. 2. Deposition inside (circles) and outside (triangles) of the holes in column II, as determined with SIMS. Dashed lines to guide the eyes. The rows are numbered in poloidal direction, see Fig. 1.

dominated one. The deposition in the three holes of each row was similar within  $\pm 12\%$ .

The line profiles of row 2 before and after exposure are shown in Fig. 3 (top), the difference between the two profiles is shown in Fig. 3 (bottom). The tile surface is curved circularly in toroidal direction in order to follow the curvature of the major radius. The fine structure of the hole bottoms is caused by the shape of the milling

cutter, which creates a conus in the hole center with a slope of about  $0.6^\circ$  and a height of  $25 \mu\text{m}$ . The grinding of the cutter edge creates the structure at the side faces of the holes. Both line profiles are overlaid in such a way, that the W-layer is at the same height in both profiles for holes I and III by taking the deposition of  $3.1 \mu\text{m}$  inside the holes, as determined by SIMS (Fig. 2), into account. We assume identical deposition in all three holes. Hole II serves for control purposes: If the W-layers of holes I and III match each other, then the W-layer in hole II also has to match. As can be seen in Fig. 3, this is the case with good precision. The limiter surface is eroded with a mean erosion of about  $20 \mu\text{m}$ , which varies only little in toroidal direction.

A two-dimensional representation of the erosion and deposition pattern on the tile is shown in Fig. 4. Row 7 was not analyzed due to the bolt holes. The dashed areas mark regions where flaking of the deposited layer is observed. The deposition in these areas cannot be determined by profilometry, because the flakes peel off the substrate. The flake thickness was determined by SEM to be about  $10 \mu\text{m}$ . This value is used in Fig. 4 for all flaking areas.

A maximum erosion of  $28 \mu\text{m}$  is observed in row 3. The erosion decreases towards the tip of the limiter and is only about  $10 \mu\text{m}$  in row 1. The transition to the deposition dominated region occurs between rows 6 and 7, except the two areas below the bolt holes, where deposition and flakes are observed. Rows 8 and 9 are deposition dominated with a maximum deposition of almost  $50 \mu\text{m}$  close to hole III in row 9 in the upper right corner

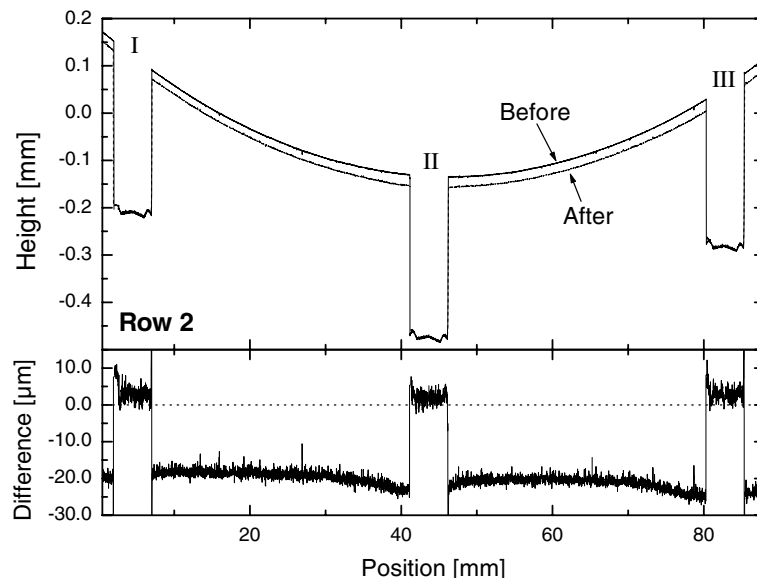


Fig. 3. Top: Line profiles of row 2 before (solid line) and after (dashed line) exposure. Bottom: Difference between the line profiles before and after exposure. The position is measured in toroidal direction.

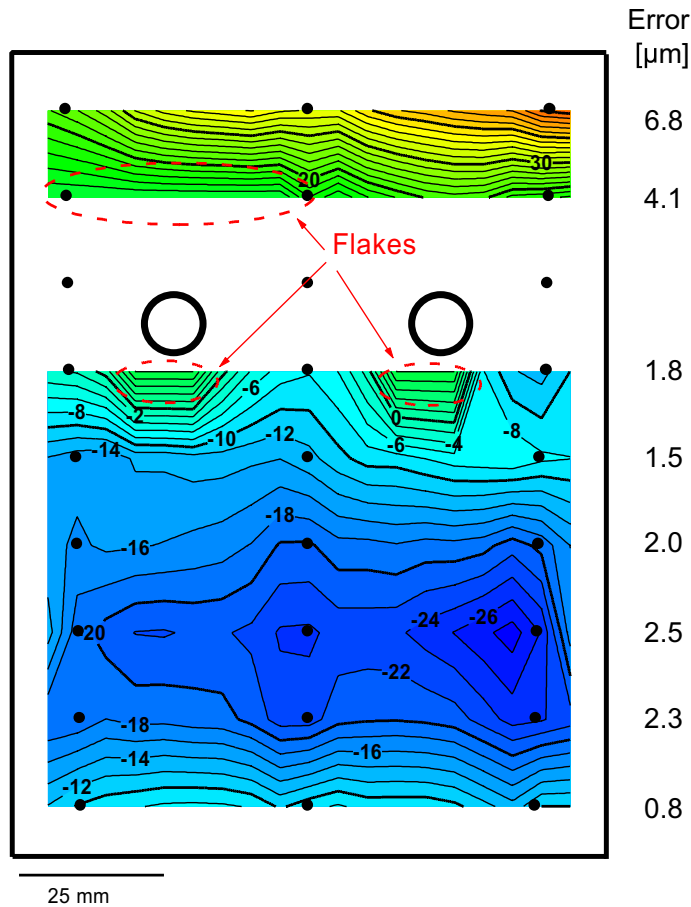


Fig. 4. Two-dimensional representation of erosion/deposition on tile 20, in  $\mu\text{m}$ , together with an error estimate in  $\mu\text{m}$  for each row. Erosion with negative sign, deposition positive. Row 7 was not analyzed. Dashed areas: Regions with flake formation, the flake thickness is assumed to be  $10 \mu\text{m}$ .

of the tile. The deposits consist mainly of carbon, with codeposited deuterium at a ratio of 0.05–0.16 D/C [6]. The boron content is typically about 5%, and metal impurities (Fe, Ni, Cr) about 1% [11]. The three boronizations are visible in the boron depth profiles, as determined with SIMS, and also in the SEM images of flakes. The deposits started to flake off the substrate after some months of storage in air. Outside of hole II in row 8 the SIMS measurement gave a deposited layer thickness of  $11.3 \pm 1.1 \mu\text{m}$ , in good agreement with SEM measurements on nearby flakes. The result from profilometry was  $11.9 \pm 3.6 \mu\text{m}$  in non-flaking areas close to the hole, in excellent agreement with SIMS and SEM. In regions where flakes peeled off the substrate the original tile surface was excavated.<sup>1</sup> In these regions the

<sup>1</sup> As could be seen in SEM pictures, the flakes detached either from the pristine surface or along the first boronization, which was applied shortly after installation of the tile.

line profiles before and after exposure agreed within  $\pm 3 \mu\text{m}$  for rows 6 and 8, which is another proof for the reliability of the method. Only for row 9 there was a disagreement between SIMS and profilometry: Outside of hole II SIMS resulted in a deposition of  $10 \mu\text{m}$ , while the deposition measured with profilometry was about  $36 \mu\text{m}$ . This may be due to partial detachment and lift-off of the deposited layer from the substrate, even if the layer visually appears well attached.

### 3.2. Error analysis

Systematic errors in the determination of the amounts of erosion/deposition result from:

(1) *Conical hole bottoms*: The bottoms of the holes are not ideally flat but conically shaped, as can be seen in Fig. 3. This cone reflects the shape of the milling cutter, the slope of the cone is  $\alpha = 0.6^\circ$ . The tip of the cone is clearly visible in a microscope, which is attached to the

profiler and allows to profile reproducibly through the center of the holes with an accuracy of  $\pm 0.025$  mm in  $y$ -direction. The maximum error  $\Delta z_1$  between two measurements is given by  $\Delta z_1 = 0.025 \text{ mm} \times \tan \alpha = 0.26 \text{ }\mu\text{m}$ .

(2) *Tilted hole bottoms*: The bottoms of the holes are not parallel to the tile surface, but tilted by an angle  $\beta$  in  $y$ -direction, i.e. perpendicular to the direction of profiling along the rows in  $x$ -direction. The angle  $\beta$  was determined for all holes by profiling along the columns in  $y$ -direction and was  $0.40$ – $5.3^\circ$ . The three holes in one row had very similar tilt angles  $\beta$ . Because the center of the holes can be met with an accuracy of  $\pm 0.025$  mm, the maximum deviation between two measurements is  $2 \times 0.025 = 0.05$  mm. The error  $\Delta z_2$  between two measurements is given by  $\Delta z_2 = 0.05 \text{ mm} \times \tan \beta$ , which gives  $\Delta z_2 = 0.4$ – $4.7 \text{ }\mu\text{m}$ .  $\beta$  was  $< 1^\circ$  for rows 1, 5 and 6, and  $> 3^\circ$  for rows 8 and 9.

(3) *Tilted tile*: The whole tile may be tilted by an angle  $\varphi$  in  $y$ -direction between the measurement before and after exposure. This is due to different attachment to the profiler table in the two measurements. The error  $\Delta z_3$  between the two measurements is given by  $\Delta z_3 = L \times \tan \varphi \times \sin \varphi$ , where  $L$  is the depth of the holes. With  $\varphi \leq 2^\circ$  and  $L$  ranging from 150 to 450  $\mu\text{m}$  this results in an error of  $\Delta z_3 = 0.2$ – $0.6 \text{ }\mu\text{m}$ .

(4) *SIMS measurement*: The thickness measurement of the deposits in the holes by SIMS has an accuracy of about 15%, resulting in an error of  $\Delta z_4 = 0.09$ – $4.9 \text{ }\mu\text{m}$ .

The nominal profiler accuracy of  $0.05 \text{ }\mu\text{m}$  is much smaller than the above error contributions. The total error  $\Delta z$  is given by the addition of the 4 error contributions, with

$$\Delta z^2 = \sum_{i=1}^4 \Delta z_i^2.$$

The largest error contributions are due to the tilt of the hole bottoms relative to the tile surface (error (2)) and the error of the SIMS measurement (error (4)). The total error is shown in Fig. 4 for each row. The smallest errors are obtained for row 1, 5 and 6 due to a small tilt angle  $\beta$  of the hole bottom towards the surface, the largest inaccuracies are observed for rows 8 and 9 due to large tilt angles  $\beta$  of  $3.5^\circ$  and  $5.3^\circ$ , and large errors from the SIMS measurements due to the thick deposits in the holes.

The accuracy of the measurement can be mainly improved by machining the holes with bottoms parallel to the surface, thus reducing error (2). However, due to the three-dimensional shape of the tile surface this is time consuming and expensive, but is applicable for flat tiles. Error (1) can be avoided by using a flat shaped milling cutter, but on the other hand the cone tip is useful for meeting the center of the holes with high accuracy, which reduces error (2). Error (3) can be reduced

by using an adapted support for the tile, which allows better mounting reproducibility.

### 3.3. Erosion and deposition on the ALT-II limiter

The observed erosion on tile 20 is about 210 mg carbon in the erosion dominated area, while about 96 mg carbon are redeposited in the deposition dominated area. The ALT-II limiter consists of 228 tiles. By assuming the investigated tile to be representative, this results in a total amount of 46 g eroded carbon from the ALT-II limiter within the exposure time of 7625 plasma seconds. This projects to a total amount of 190 kg eroded carbon, with a maximum erosion rate of about 12 cm, in 1 burn year. The eroded carbon is partly redeposited in the deposition dominated area of the ALT-II limiter (about 21.5 g carbon on the whole ALT-II limiter within the exposure time). The rest is either deposited on areas in the scrape-off layer perpendicular to the magnetic field [1,3,12,13], on the neutralizer plates of the pumped limiter [1], in the pump ducts [1,14], or is pumped out as hydrocarbon gas, mainly  $\text{CD}_4$ . The balance of eroded and deposited carbon in TEXTOR is subject of a different paper [15].

## 4. Conclusions

A new method using optical profilometry has been developed for the determination of massive erosion and deposition on plasma facing components. The method was tested successfully on a graphite tile of the ALT-II limiter of TEXTOR. The bottoms of machined holes serve as stable reference points, a hole depth of 0.1 mm is already sufficient to convert a net erosion to a net redeposition zone. An accuracy of about  $1 \text{ }\mu\text{m}$  can be achieved by this method, if the hole bottoms are oriented parallel to the tile surface. Combination with SIMS or ion beam analysis methods is essential due to deposition in the holes.

After exposure for 7625 plasma seconds a maximum erosion of  $28 \text{ }\mu\text{m}$  carbon is observed in erosion dominated areas of the tile, while a maximum deposition of  $40 \text{ }\mu\text{m}$  is observed in net redeposition areas. The ability to determine erosion and not only deposition on plasma exposed surfaces enables new insight into the sources of eroded material and the global carbon balance.

## Acknowledgement

Sputter deposition of tungsten inside the holes was performed by H.J. Bierfeld from IFF/FZ Jülich, whose help is gratefully acknowledged.

## References

- [1] M. Mayer, V. Philipps, P. Wienhold, H.G. Esser, J. von Seggern, M. Rubel, J. Nucl. Mater. 290–293 (2001) 381.
- [2] G. Federici, R. Anderl, P. Andrew, J.N. Brooks, R.A. Causey, J.P. Coad, D. Cowgill, R.P. Doerner, A.A. Haasz, G. Janeschitz, W. Jacob, G.R. Longhurst, R. Nygren, A. Peacock, M.A. Pick, V. Philipps, J. Roth, C.H. Skinner, W.R. Wampler, J. Nucl. Mater. 266–269 (1998) 14.
- [3] M. Rubel, J. von Seggern, P. Karduck, V. Philipps, A. Vevecka-Priftaj, J. Nucl. Mater. 266–269 (1999) 1185.
- [4] J. von Seggern, M. Rubel, P. Karduck, V. Philipps, H.G. Esser, P. Wienhold, Phys. Scr. T 81 (1999) 31.
- [5] M. Mayer, R. Behrisch, K. Plamann, P. Coad, P. Andrew, A.T. Peacock, J. Nucl. Mater. 266–269 (1999) 604.
- [6] M. Rubel, P. Wienhold, D. Hildebrandt, J. Nucl. Mater. 290–293 (2001) 473.
- [7] P. Wienhold, F. Weschenfelder, J. von Seggern, B. Emmoth, H.G. Esser, P. Karduck, J. Winter, J. Nucl. Mater. 241–243 (1997) 804.
- [8] M. Mayer, R. Behrisch, P. Andrew, A.T. Peacock, J. Nucl. Mater. 241–243 (1997) 469.
- [9] G.M. McCracken, D.H.J. Goodall, P.C. Stangeby, J.P. Coad, J. Roth, B. Denne, R. Behrisch, J. Nucl. Mater. 162–164 (1989) 356.
- [10] A.W. Koch, M. Ruprecht, R. Wilhelm, Laser speckle techniques for in situ – monitoring of erosion and redeposition at inner walls in large experimental fusion devices. Tech. Rep. IPP4/271, Max-Planck-Institut für Plasmaphysik, 1995.
- [11] P. Wienhold, H.G. Esser, D. Hildebrandt, A. Kirschner, K. Ohya, V. Philipps, M. Rubel, J. von Seggern, Phys. Scr. T 81 (1999) 19.
- [12] P. Wienhold, F. Weschenfelder, P. Karduck, K. Ohya, S. Richter, J. von Seggern, J. Nucl. Mater. 266–269 (1999) 986.
- [13] P. Wienhold, H.G. Esser, D. Hildebrandt, A. Kirschner, M. Mayer, V. Philipps, M. Rubel, J. Nucl. Mater. 290–293 (2001) 362.
- [14] J. von Seggern, P. Wienhold, T. Hirai, V. Philipps, these Proceedings. [PII: S0022-3115\(02\)01411-3](#).
- [15] P. Wienhold et al., these Proceedings. [PII: S0022-3115\(02\)01347-8](#).